NVP-BEZ235, a Dual PI3K/mTOR Inhibitor, Prevents PI3K Signaling and Inhibits the Growth of Cancer Cells with Activating PI3K Mutations

Violeta Serra, Ben Markman, Maurizio Scaltriti, Pieter J.A. Eichhorn, Vanesa Valero, Marta Guzman, Maria Luisa Botero, Elisabeth Llonch, Francesco Atzori, Serena Di Cosimo, Michel Maira, Carlos Garcia-Echeverria, Josep Lluis Parra, Joaquin Arribas, and José Baselga

[1]Laboratory of Oncology Research, Medical Oncology Service, and [2]Department of Pathology, Vall d'Hebron University Hospital, Barcelona, Spain; and [3]Novartis Institutes for BioMedical Research-Novartis Oncology, Basel, Switzerland

Abstract

Phosphatidylinositol-3-kinase (PI3K) pathway deregulation is a common event in human cancer, either through inactivation of the tumor suppressor phosphatase and tensin homologue deleted from chromosome 10 or activating mutations of p110-α. These hotspot mutations result in oncogenic activity of the enzyme and contribute to therapeutic resistance to the anti-HER2 antibody trastuzumab. The PI3K pathway is, therefore, an attractive target for cancer therapy. We have studied NVP-BEZ235, a dual inhibitor of the PI3K and the downstream mammalian target of rapamycin (mTOR). NVP-BEZ235 inhibited the activation of the downstream effectors Akt, S6 ribosomal protein, and 4EBP1 in breast cancer cells. The antiproliferative activity of NVP-BEZ235 was superior to the allosteric selective mTOR complex inhibitor everolimus in a panel of 21 cancer cell lines of different origin and mutation status. The described Akt activation due to mTOR inhibition was prevented by higher doses of NVP-BEZ235. NVP-BEZ235 reversed the hyperactivation of the PI3K/mTOR pathway caused by the oncogenic mutations of p110-α, E545K, and H1047R, and inhibited the proliferation of HER2-amplified BT474 cells exogenously expressing these mutations that render them resistant to trastuzumab. In trastuzumab-resistant BT474 H1047R breast cancer xenografts, NVP-BEZ235 inhibited PI3K signaling and had potent antitumor activity. In treated animals, there was complete inhibition of PI3K signaling in the skin at pharmacologically active doses, suggesting that skin may serve as surrogate tissue for pharmacodynamic studies. In summary, NVP-BEZ235 inhibits the PI3K/mTOR axis and results in antiproliferative and antitumoral activity in cancer cells with both wild-type and mutated p110-α. [Cancer Res 2008;68(19):8022–30]

Introduction

The phosphatidylinositol-3-kinase (PI3K)/Akt signaling pathway plays a central role in diverse cellular functions, including proliferation, growth, survival, and metabolism. In addition to their physiologic role, several isoforms of the PI3K family are implicated in pathologic processes and diseases. In particular, members of class 1A PI3Ks, which are heterodimers comprised of a p85 regulatory and a p110 catalytic subunit, are often mutated in human cancer (1–6).

The initiating event of a growth factor binding to a receptor tyrosine kinase enables PI3K to interact with the intracellular domain of the receptor tyrosine kinase (7, 8). This binding, which occurs either directly or indirectly via adaptor molecules such as insulin receptor substrate 1 (IRS-1), removes the inhibitory effect of p85 and leads to the activation of the lipid kinase activity of the p110 subunit (9). The GTPase RAS can also directly activate PI3K (10). p110 phosphorylates the phosphatidylinositol-4,5-diphosphate to phosphatidylinositol-3,4,5-triphosphate, itself responsible for facilitating the phosphorylation of Akt (also known as PKB) at Thr308 by PDK1 (11). A second phosphorylation event at Ser473 by the mammalian target of rapamycin (mTOR)-rictor complex (mTORC2) is required for maximal Akt activity (8, 12).

Akt is the central effector of the pathway (reviewed in Engelman and colleagues 13). It is able to execute its myriad cellular operations via a host of effectors, including direct substrates such as tuberous sclerosis 2 (TSC2), glycogen synthase kinase 3 (GSK3), and the forkhead box transcription factors (FOXO). It promotes protein synthesis and cell growth by alleviating TSC1/2 suppression of mTOR, allowing the latter to act as part of the mTOR-raptor complex on 4EBP1 and ribosomal protein S6 kinases (S6K; ref. 14). Akt reduces cell cycle inhibitors p27 and p21, and promotes cell cycle proteins c-Myc and cyclin D1, resulting in enhanced cellular proliferation. Influence extends to a host of proapoptotic and antiapoptotic proteins, such as the Bcl-2 family member Bad, limiting programmed cell death and boosting cellular survival. Some of these phenomena are mediated by the Akt-driven expulsion of FOXO from the nucleus, from which it normally inhibits the transcription of genes promoting apoptosis and cell cycle arrest.

Genetic aberrations of the PI3K/Akt pathway are among the most commonly encountered in human cancer. Germ line loss of function mutations at the *PTEN* gene locus on chromosome 10q result in cancer predisposition syndromes, whereas somatic loss of heterozygosity 10q is prevalent in breast, gastric, endometrial and prostate cancer, and glioblastomas (13, 15). *PIK3CA*, the gene encoding p110-α, is frequently amplified or mutated. The mutations tend to cluster in "hotspots", with ~80% accounted for by oncogenic substitutions in exon 9 (E542K and E545K) and exon 20 (H1047R; ref. 1). Breast, colon, endometrial, and hepatocellular cancers harbor these changes with greatest frequency in human populations (16). These critical perturbations have shown transforming capacity *in vitro* and *in vivo* (17, 18).

Note: Supplementary data for this article are available at Cancer Research Online (http://cancerres.aacrjournals.org/).

Requests for reprints: José Baselga, Vall d'Hebron University Hospital, Passeig Vall d'Hebron 119, 08035 Barcelona, Spain. Phone: 34-9327-46085; Fax: 34-9327-46059; E-mail: jbaselga@vhebron.net.

doi:10.1158/0008-5472.CAN-08-1385

Excessive signaling through the PI3K/Akt cascade has been shown to be both prognostic and predictive. In breast cancer, *PIK3CA* mutation and functional PTEN loss have been linked with poorer patient outcomes, whereas in glioblastoma, high pathway activity has been shown to be significantly associated with reduced patient survival times (19, 20). Constitutive PI3K activity predicting for resistance to cytotoxic agents has been shown in models of breast, lung, and ovarian cancer, often evidenced by attenuation in the level of apoptosis (21–23). Furthermore, the anti-HER2 monoclonal antibody trastuzumab depends on intact p110-α or PTEN for its action in HER2-overexpressing breast cell lines (19, 24).

This constellation of features of PI3K/Akt signaling—critical cellular functions, prevalent oncogenic genetic aberrations, consequent therapeutic resistance, and its potential reversal—have made the inhibition of this pathway an attractive target for developmental anticancer strategies. A new generation of PI3K inhibitors is emerging, overcoming earlier problems of poor selectivity, unfavorable pharmacokinetic profiles, and unacceptable toxicity (reviewed in ref. 25). A number of these agents have entered early phase clinical trials. NVP-BEZ235 (Novartis Pharma) is a synthetic low molecular mass compound belonging to the class of imidazoquinolines that potently and reversibly inhibits class 1 PI3K catalytic activity by competing at its ATP-binding site. NVP-BEZ235 also inhibits mTOR catalytic activity but does not target other protein kinases (26).

In this report, we show that NVP-BEZ235 is highly active against breast cancer cell lines and xenografts harboring endogenous or overexpressed p110-α mutants. Under the tested experimental conditions, we establish a differential effect of NVP-BEZ235 according to the concentration used, whereby mTOR inhibition predominates at a low concentration (<100 nmol/L) but dual mTOR/PI3K blockade is observed at relatively higher concentrations (≈500 nmol/L).

Materials and Methods

Cell lines and treatments. All the cell lines were obtained from the American Type Culture Collection and maintained in 1:1 DMEM/F12 supplemented with 10% fetal bovine serum and 2 mmol/L L-glutamine (Life Technologies, Inc. Ltd.) at 37°C in 5% CO_2. Cells infected with the PI3K-based vectors were selected and maintained in the same medium containing 1.0 and 0.5 μg/mL of puromycin (Sigma), respectively. NVP-BEZ235, everolimus (NVP-RAD001), and NVP-AEW541 were kindly provided by Novartis Institutes for BioMedical Research-Oncology, Basel Switzerland and were dissolved in DMSO. Trastuzumab (Herceptin; kindly provided by F. Hoffmann-La Roche, Basel, Switzerland) was dissolved in sterile apyrogenic water. Cells were treated at the indicated final concentrations of drugs. Wherever indicated, cells were serum-deprived for 16 h, then incubated with the appropriate inhibitor, and finally stimulated with insulin growth factor I (IGF-I; 50 ng/mL) for 30 min. DMSO was added to the culture medium of the control cells and was always kept below 0.1%.

Western blot, immunoprecipitation, and immunofluorescence. For drug treatments, cells were counted and their viability assessed with a Guava cytometer. Cells (2×10^5 to 4×10^5) were grown in 60 mm dishes and treated with NVP-BEZ235 for the indicated concentrations and time. Cells were washed twice with ice-cold PBS and scraped into ice-cold radioimmunoprecipitation assay lysis buffer (20 mmol/L Na_2PO_4, 150 mmol/L NaCl, 5 mmol/L EDTA, 1% Triton X-100, 25 mmol/L β-glycerol phosphate, 1 mmol/L $MgCl_2$, 50 mmol/L NaF supplemented with 200 μmol/L Na_2VO_4, and protease inhibitor cocktail; Roche). For detection of caspase 3 and poly(ADP-ribose)polymerase (PARP) cleavage products, the detached cells were collected and lysed together with the adherent cells. Lysates were cleared by centrifugation at 15,000 × *g* for 10 min at 4°C, and supernatants were then removed and assayed for protein concentration using the DC Protein assay (Bio-Rad). Thirty micrograms of total lysates were resolved by SDS-PAGE, and electrophoretically transferred to nitrocellulose or polyvinylidene difluoride (for Thr308-P-Akt, 4EBP1 and cleaved caspase 3 detection) membranes. Membranes were hybridized with the following primary antibodies from Cell Signaling: Ser473-P-Akt, Thr308-P-Akt, Akt, Ser240/244-P-S6, S6, 4EBP1, PARP, IRS-1, and cleaved caspase 3 in 5% bovine serum albumin or with caspase 3 (Alexis Biochemicals) and actin (Bionova) in 1% nonfat dry milk. Mouse and rabbit horseradish peroxidase–conjugated secondary antibodies (Amersham Biosciences) were used at 1:3,000 in PBS-T/1% nonfat dry milk. Protein-antibody complexes were detected by chemiluminescence with the SuperSignal West Dura Extended Duration Substrate, and images were captured with a FUJIFILM LAS-3000 camera system. The experiments were repeated at least thrice.

For immunoprecipitation experiments, cells were grown in 100 mm dishes and treated with NVP-BEZ235, everolimus, NVP-AEW541, or the combination of drugs for 24 to 48 h. Volumes of 500 μL of lysis buffer containing equal amount of proteins were incubated with immobilized Akt1 antibody (Cell Signaling) overnight at 4°C with gentle rotation. The beads were washed thrice with lysis buffer before suspension in SDS loading buffer. For immunofluorescence, 4×10^4 cells were seeded on 14-mm coverslips in 24-well plates. After treatment was completed, cells were washed with PBS, fixed in 4% paraformaldehyde-PBS for 20 min at room temperature and permeabilized in cold PBS with 0.2% Triton X-100 for 10 min at room temperature. After blocking with PBS, 1% bovine serum albumin, 0.1% saponin, and 0.02% azide for 40 min at room temperature, the slides were incubated with the primary antibody (1:50, FOXO; Santa Cruz) for 1 h at room temperature and thereafter with the anti-rabbit Alexa 488 antibody (1:500). Coverslips were mounted on glass slides with 4′,6-diamidino-2-phenylindole–containing Vectashield mounting medium (Vector Laboratories) and visualized by confocal microscopy. The negative control shows a staining without primary antibody.

Cell cycle analysis. Cells (5×10^5) were seeded in 60-mm dishes and treated with NVP-BEZ235 for 48 h. Floating and adherent cells were collected by trypsinization and washed once with PBS. Cells were incubated in 70% ethanol at −20°C overnight, treated with 20 μg/mL RNase A, then stained with 0.5 μg/mL of propidium iodide, and evaluated by flow cytometry (Beckman Coulter Epics XL, Beckman Coulter). The experiments were repeated thrice.

Proliferation assays: crystal violet and WST-1. Depending on the cell line, 2×10^3 to 4×10^5 cells were seeded in six-well plates and treated with increasing doses of NVP-BEZ235. Medium was replaced every 3 to 4 days. After 11 days, adherent cells were fixed in 20% glutaraldehyde in growth medium for 10 min, then washed twice in distilled water and stained with 0.1% crystal violet for 30 min. After washing, the stain was dissolved with 10% acetic acid and subsequently quantified at 570 nm. The 50% growth-inhibitory concentrations were calculated for at least two independent assays per cell line. For BT474 cells overexpressing the ecotropic receptor (BT474-eco), 4×10^4 cells were seeded in 12-well plates. Medium was replaced every 3 to 4 days with the indicated drugs. After 8 days, cell proliferation was quantified by crystal violet as described.

For WST-1–based cell viability assays, 1×10^5 cells were seeded in 96-well plates and were treated with increasing doses of NVP-BEZ235 and everolimus for 72 h, starting 24 h after seeding (day 1). The WST-1 colorimetric assay was quantified at 415 nm, and normalized to the value of untreated cells. A duplicate plate of untreated cells was measured at 24 h. The *X*-axis value represents the amount of cells at the beginning of the assay and resulted from the ratio between untreated cells at 24 h and untreated cells at 72 h. All experiments were repeated at least twice.

Overexpression of *PIK3CA* mutants. pBABE-based and pJp-1520–based vectors were kindly provided by Marion Dorsch (Novartis Oncology, Cambridge, MA) and Joan Brugge (Harvard Medical School, Boston, MA), respectively. Plasmid DNA was sequenced to confirm the presence of the oncogenic mutations. SkBr3 and BT474 cells overexpressing the ecotropic receptor (SkBr3-eco and BT474-eco, respectively) were infected with ecotropically packed retroviruses, whereas amphotropic viruses were needed to infect MDA-231 and BT474-VH2 cells.

Tumor xenografts in nude mice. Mice were maintained and treated in accordance with institutional guidelines of Vall d'Hebron University Hospital Care and Use Committee. Six- to 8-week-old female athymic nude-*Foxn1*^{nu} mice were purchased from Harlan Laboratories (Italy). Mice were housed in air-filtered laminar flow cabinets with a 12-h light cycle and food and water *ad libitum*. Mice were handled with aseptic procedures and allowed to acclimatize to local conditions for 1 week before the experimental manipulations. A 17β-estradiol pellet (Innovative Research of America) was implanted s.c. into each mouse 1 day before injection of BT474-VH2 cells. BT474-VH2 cells were obtained from *in vitro* explants of BT474-derived xenografts (27) and expanded in DMEM/F12 supplemented with 10% fetal bovine serum, 0.5 μg/mL puromycin (Sigma), and 2 mmol/L of L-glutamine at 37°C in 5% CO_2. Cells (2×10^7) were resuspended in PBS, mixed with Matrigel (1:1; BD Biosciences) and injected s.c. into the right flank of each mouse in 200 μL of final volume. Treatment began when tumors reached an average size of 500 mm^3 (11 days after injection) and were thus considered as established growing xenografts. NVP-BEZ235 (40 mg/kg in 10% NMP–90% PEG) was freshly prepared and given p.o. once every 24 h in 100 μL of volume. Tumor xenografts were measured with calipers thrice a week, and tumor volume was determined using the formula: (length × width^2) × (π/6). At the end of the experiment, the animals were anesthetized with a 1.5% isofluorane-air mixture and killed by cervical dislocation. Results are presented as mean ± SD.

Immunohistochemistry. Tumor xenografts and non–tumor tissue (skin) were fixed immediately after removal in a 10% buffered formalin solution for a maximum of 48 h at room temperature before being dehydrated and paraffin-embedded under vacuum conditions. Slides were deparaffinized, and endogenous peroxidase activity was blocked by incubation in 3% H_2O_2 in methanol for 10 min at room temperature. Sections were then microwaved in PBS for 4 min for antigen retrieval and incubated with avidin and then biotin for 15 min each to block nonspecific binding. An immunoperoxidase technique was then performed using a

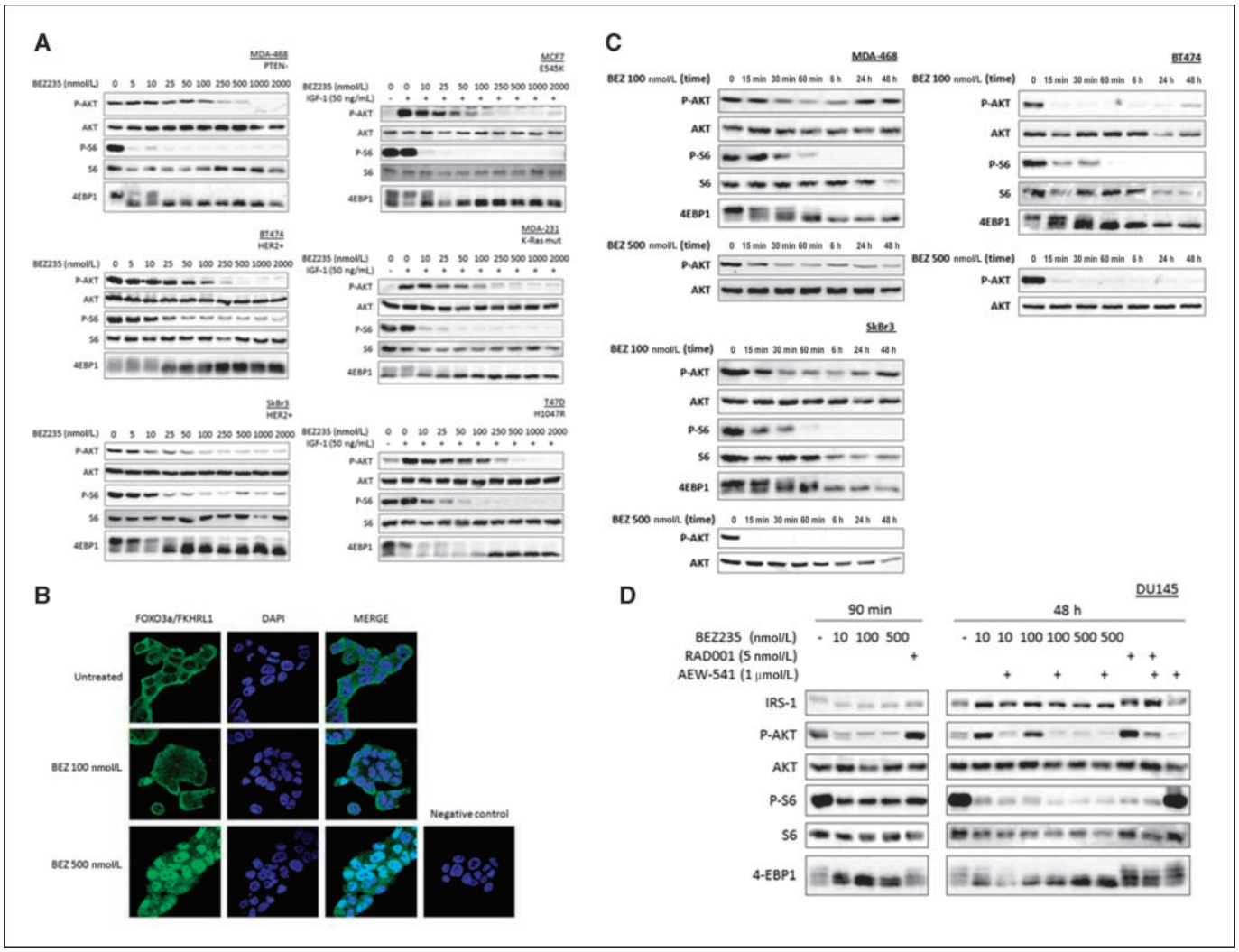

Figure 1. NVP-BEZ235 inhibits the PI3K pathway. *A,* Western blot showing decrease in Ser473-P-Akt, Ser240/244-P-S6, and of P-4EBP1 (lower mobility shift) in total lysates from breast cancer cells treated with NVP-BEZ235 for 6 h at the indicated concentrations ranging from 0 to 2,000 nmol/L. Total Akt and S6 levels are shown for loading control. Where indicated, cells were serum-starved then stimulated with IGF-I. *B,* immunofluorescence showing nuclear relocalization of endogenous FOXO3a/FKHRL1 in BT474 cells treated with NVP-BEZ235 at 100 and 500 nmol/L for 6 h. *C,* Western blot of total lysates of SkBr3, BT474 and MDA-468 cells treated with NVP-BEZ235 at concentrations 100 and 500 nmol/L for up to 48 h. Phosphorylation of Akt initially decreased but slowly recovered after 24 h to 48 h, whereas S6 remained dephosphorylated, as did 4EBP1. At 500 nmol/L, NVP-BEZ235 inhibition of Akt phosphorylation was sustained. *D,* Western blot of total lysates showing increase in Akt phosphorylation in DU145 cells treated with NVP-BEZ235 at 10 and 100 nmol/L and everolimus at 5 nmol/L for 48 h. AEW-541 (1 μmol/L) prevented both NVP-BEZ235-dependent and everolimus-dependent increase in the phosphorylation of Akt. NVP-BEZ235 (500 nmol/L) fully decreased P-Akt. As a control, 90 min of treatment with the dual inhibitor fully decreased P-Akt, P-S6, and P-4EBP1. Everolimus (5 nmol/L) did not fully dephosphorylate 4EBP1. NVP-BEZ235 induced IRS-1 dephosphorylation (lower mobility shift) and accumulation, similar to everolimus.

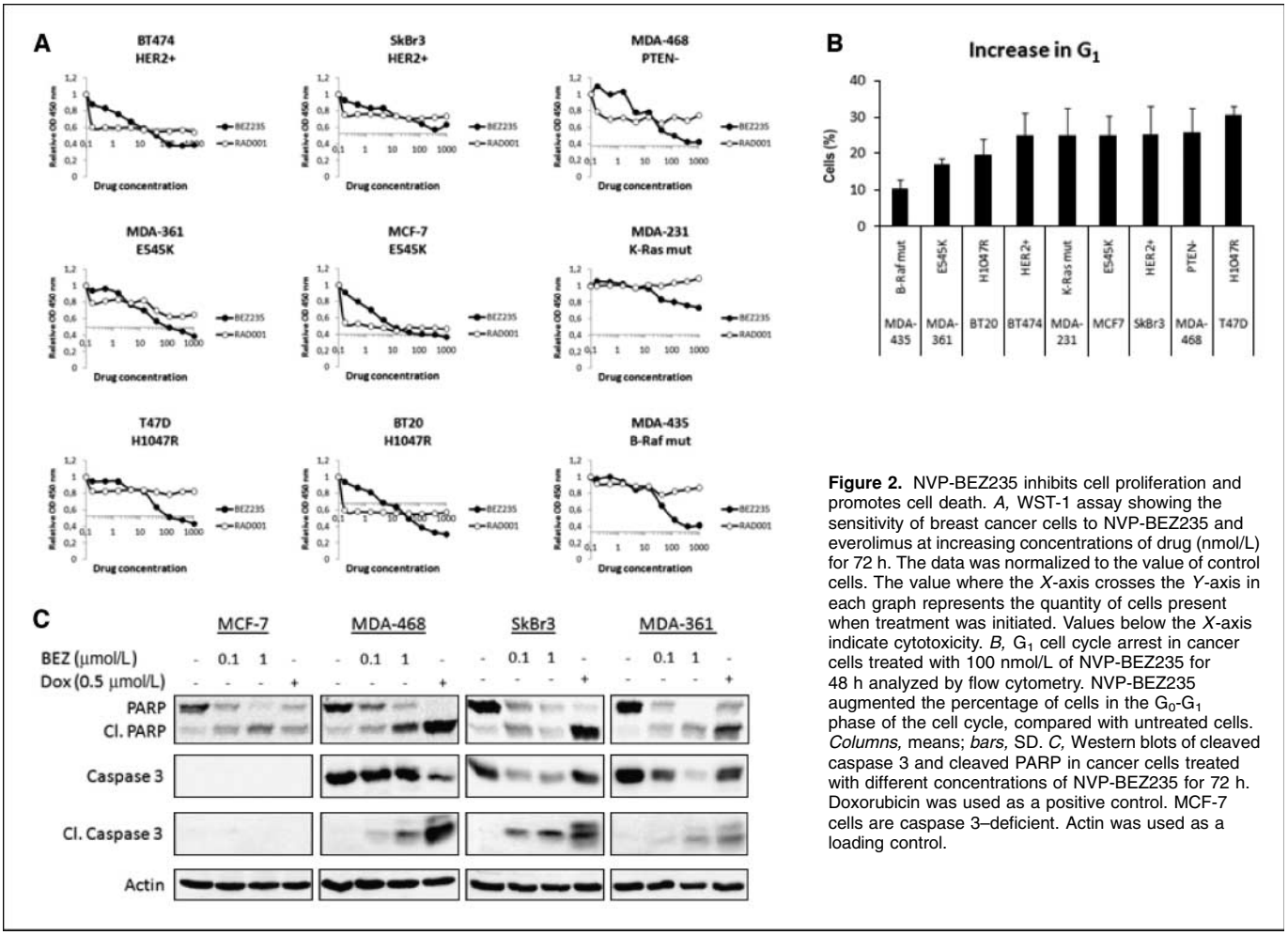

Figure 2. NVP-BEZ235 inhibits cell proliferation and promotes cell death. *A,* WST-1 assay showing the sensitivity of breast cancer cells to NVP-BEZ235 and everolimus at increasing concentrations of drug (nmol/L) for 72 h. The data was normalized to the value of control cells. The value where the *X*-axis crosses the *Y*-axis in each graph represents the quantity of cells present when treatment was initiated. Values below the *X*-axis indicate cytotoxicity. *B,* G_1 cell cycle arrest in cancer cells treated with 100 nmol/L of NVP-BEZ235 for 48 h analyzed by flow cytometry. NVP-BEZ235 augmented the percentage of cells in the G_0-G_1 phase of the cell cycle, compared with untreated cells. *Columns,* means; *bars,* SD. *C,* Western blots of cleaved caspase 3 and cleaved PARP in cancer cells treated with different concentrations of NVP-BEZ235 for 72 h. Doxorubicin was used as a positive control. MCF-7 cells are caspase 3–deficient. Actin was used as a loading control.

commercial kit (Vectastain ABC Elite, Vector Laboratories). Primary antibodies were Ser473-P-Akt, Ser240/244-P-S6, Thr70-P-4EBP1, and Ki67 (all from Cell Signaling) and secondary antibody was from Amersham. As a negative control, primary antibody was omitted. No labeling was ever observed in control experiments when primary antibodies were omitted or, alternatively, when normal nonimmune serum was used. There was no evidence of cross-reactivity with the antibodies used in this study. H-scores were used to quantify the expression of the phosphoproteins, whereas the percentage of stained cells was counted in the Ki67 staining.

Statistical analysis. Inhibitory concentrations 50 (IC_{50}) and growth-inhibitory concentrations 50 (GI_{50}) were estimated graphically as the concentration of drug that inhibited the phosphoprotein levels to 50% of control cells or the drug concentration that inhibited cell growth by 50%. For *in vitro* assays and nude mice experiments, comparisons between groups were made using a two-tailed Student's *t* test. Differences of $P < 0.05$ were considered statistically significant.

Results

NVP-BEZ235 inhibits Akt, S6RP (S6), and 4EBP1 phosphorylation and induces FKHRL1 nuclear translocation. The dual p110 and mTORC1/2 inhibitory activity of NVP-BEZ235 was assessed in breast cancer cell lines with different modulations of the PI3K/Akt cascade as a result of wild-type p110-α (MDA-231), mutated p110-α (MCF7, T47D), loss of PTEN (MDA-468), or amplification of HER2 (BT474, SkBr3). Dose-response experiments showed that NVP-BEZ235 was able to inhibit the phosphorylation of Ser473-Akt, Ser240/244-S6, and 4EBP1 in all cell lines tested, irrespective of the basal activation of PI3K/Akt cascade (Fig. 1*A*). Similar findings were observed in a panel of non–breast cancer cell lines (data not shown). Together with Ser473-P-Akt, phosphorylation of Thr308-Akt was also reduced in a dose-dependent manner (Supplementary Fig. S1). Of note, the IC_{50} for Ser473-P-Akt was 6.4-fold higher than that of P-S6 (77 ± 29 nmol/L compared with 12 ± 10 nmol/L). In agreement with an elevated IC_{50} for Ser473-P-Akt, we observed that complete FKHRL1 nuclear translocation was achieved only at 500 nmol/L NVP-BEZ235 and not at the lower dose of 100 nmol/L (Fig. 1*B*).[4] Indeed, mTORC2 is the necessary component of the Ser473-P-Akt-FOXO pathway (28).

Moreover, time course experiments revealed that long-term exposure to low concentrations of NVP-BEZ235 resulted in sustained inhibition of P-S6, with a concomitant increase of P-Akt levels. Such an effect on P-Akt was completely abolished in cells incubated at higher concentrations of the inhibitor (Fig. 1*C*). In agreement with previously published data (29, 30), we found that the total levels of S6 decreased after long-term exposure to NVP-BEZ235.

[4] M. Maira, unpublished data.

Suboptimal doses of NVP-BEZ235 induce Akt phosphorylation. We investigated whether the long-term increase in P-Akt levels observed in cells exposed to a low concentration of NVP-BEZ235 was due to the disruption of the known S6K1 to IRS-1 negative feedback loop (31). For this purpose, we chose the DU145 prostate cancer cells, for which the rapamycin-induced deregulation of S6K–IRS-1 is well described (32). When DU145 cells were treated with NVP-BEZ235 for a short period of time (90 minutes) Akt was completely dephosphorylated regardless of the dose level used (Fig. 1*D*). On the contrary, as previously observed in Fig. 1*C*, longer term (48 hours) exposure to low doses of NVP-BEZ235 (10 and 100 nmol/L) induced an increase in P-Akt. This effect was prevented by the IGF-IR tyrosine kinase inhibitor AEW-541. Also, a higher NVP-BEZ235 concentration (500 nmol/L) completely blocked Akt phosphorylation in these cells, irrespective of treatment duration. As expected, the rapamycin analogue everolimus, an mTORC1 inhibitor (which seems to have additional activity against the mTORC2 in some cells; ref. 33) led to the inactivation of mTOR targets and was associated with increased levels of P-Akt both at 90 minutes and 48 hours. This effect was abolished by NVP-AEW541 (48 hours). Both inhibitors, NVP-BEZ235 and everolimus, induced IRS-1 dephosphorylation (lower mobility shift) and accumulation, as described for everolimus (32). Although a similar effect was observed in the breast cancer cell lines BT474 and MDA-468, this was not reverted with the help of IGF-IR (Supplementary Fig. S2).

Reduction of cellular proliferation in cancer cells is associated with G_1 arrest and induction of apoptosis. Cellular viability and proliferation was assessed by both WST-1 assay and crystal violet staining in an extended panel of cancer cells of different origin with diverse activation status in the PI3K and Ras pathways (n = 21). NVP-BEZ235 reduced the number of viable cells in a dose-dependent manner in all cell lines tested after 3 days (Fig. 2*A*; Supplementary Fig. S3). When compared with everolimus, the dual inhibitor NVP-BEZ235 was consistently more potent in inhibiting the proliferation of the tested cells at concentrations >10 nmol/L. Similar results were obtained by treating the cancer cells for an extended period of time and calculating the GI_{50}s. All cells tested were potently inhibited by NVP-BEZ235, with GI_{50}s ranging between 5 and 32 nmol/L. A trend was observed, in that K-Ras/B-Raf/EGFR+ cell lines were less sensitive to NVP-BEZ235 (Supplementary Fig. S4).

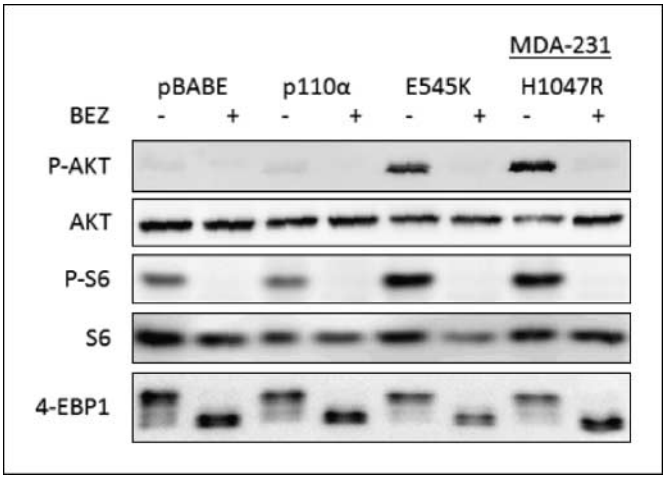

Figure 3. NVP-BEZ235 is active against the p110-α hotspot mutations. Western blot of total lysates of MDA-231 cells engineered to overexpress either wild-type or the oncogenic mutations of p110-α (E545K and H1047R). E545K- and H1047R-overexpressing cells had higher levels of p-Akt compared with mock control or p110-α–overexpressing cells. The increased Akt phosphorylation was inhibited by 100 nmol/L of NVP-BEZ235 treatment for 6 h.

Consistent with the antiproliferative effects of NVP-BEZ235, the proportion of cells in the G_1 phase of the cell cycle was substantially increased after treatment with the inhibitor (Fig. 2*B*). Markers of apoptosis such as cleavage products of caspase 3 and PARP were detected by Western blot in four representative breast cancer cell lines with different PI3K pathways and HER2 status (Fig. 2*C*).

NVP-BEZ235 targets p110-α oncogenic mutations. In order to confirm the ability of NVP-BEZ235 to target the p110-α oncogenic mutations in cell culture, we exogenously expressed wild-type p110-α and the E545K and H1047R mutations in a cell line with a wild-type p110-α background and low levels of basal P-Akt (MDA-231 cells). In conditions of serum deprivation, the oncogenic mutations induced constitutive Akt phosphorylation, which was abolished when the cells were treated with NVP-BEZ235 for 6 hours (Fig. 3), demonstrating that NVP-BEZ235 targets p110-α oncogenic mutations.

NVP-BEZ235 overcomes trastuzumab-resistance driven by p110-α oncogenic mutations in HER2-positive breast cancer cells. We engineered both BT474 and SkBr3 breast cancer cells (HER2-amplified and trastuzumab-sensitive) to overexpress the p110-α–activating mutations E545K or H1047R, which have recently been shown to confer resistance to trastuzumab (19). As expected, overexpression of mutated p110-α E545K and H1047R in BT474 cells increased P-Akt when compared with control cells (Fig. 4*A*). Down-regulation of HER2 with trastuzumab reduced the levels of Akt in control cells but not in wild-type or mutated p110-α–overexpressing cells. Similarly, 4EBP1 was dephosphorylated only in control cells treated with trastuzumab. NVP-BEZ235 was active in decreasing Akt, S6, and 4EBP1 phosphorylation in all cells regardless of their p110-α status. A WST-1 assay was used to assess the growth-inhibitory potential of both trastuzumab and NVP-BEZ235 at increasing doses. BT474 cells bearing p110-α oncogenic mutations were less sensitive to trastuzumab compared with the p110-α wild-type and control cells (Fig. 4*B*). The capacity of NVP-BEZ235 to inhibit the proliferation of p110-α–mutated cells was also quantified by crystal violet staining after 8 days of continuous drug exposure. Hotspot mutated cells grew faster than control cells in the presence of trastuzumab, whereas all cells showed equal growth inhibition in the presence of NVP-BEZ235 (Fig. 4*C*). The same effects as in Fig. 4*A, B* and *C* were observed in SkBr3 cells overexpressing the PI3K mutants (data not shown).

NVP-BEZ235 antitumor activity *in vivo*. The antitumor activity of NVP-BEZ235 was further studied in a xenograft model derived from HER2-amplified BT474 breast cancer cells engineered to express either the H1047R hotspot mutation or the empty vector (pBABE). NVP-BEZ235 daily oral treatment at 40 mg/kg started 11 days after cell injection, when tumors reached an average volume of 500 mm^3. NVP-BEZ235 resulted in suppressed tumor growth (Fig. 5*A*). The H1047R-overexpressing tumors responded better to the NVP-BEZ235 treatment when compared with mock controls. At the end of the experiment, we measured the levels of P-Akt, P-S6, P-4EBP1, and Ki67 in tumor tissues by Western blot and immunohistochemistry excised from the mice at 1 and 24 hours post-drug administration. In both H1047R and control tumors,

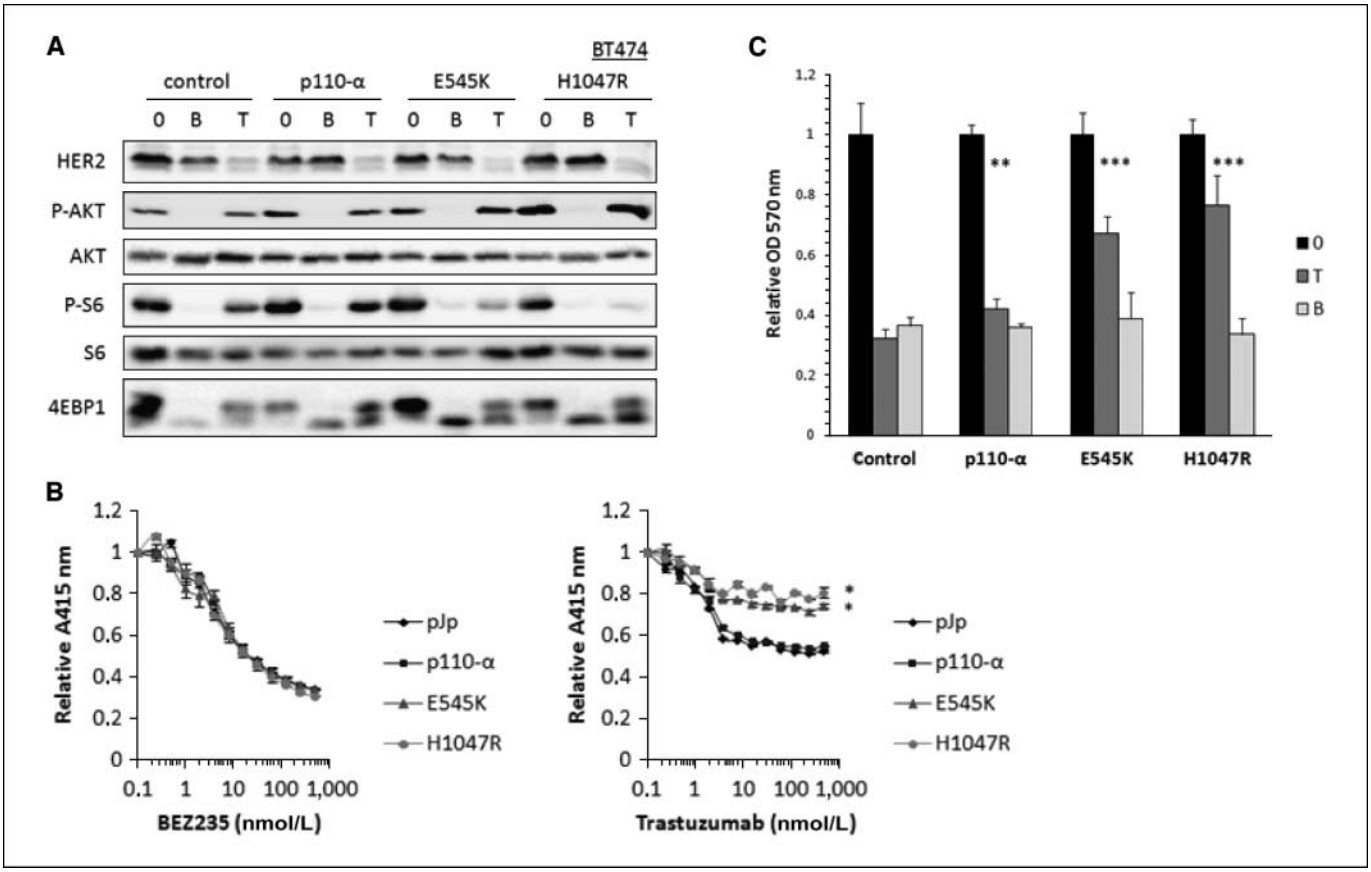

Figure 4. PI3K mutants in HER2+ cells are sensitive to NVP-BEZ235 *in vitro. A,* overexpression of E545K and H1047R mutations induced Akt phosphorylation in untreated cells (*O*). Trastuzumab (*T,* 50 nmol/L, 48 h) decreased HER2 expression in all cells treated but only achieved Akt and 4EBP1 dephosphorylation in control cells. NVP-BEZ235 (*B,* 500 nmol/L, 24 h) achieved dephosphorylation of all of the depicted PI3K targets in all cells. *B,* the sensitivity of BT474 cells overexpressing either p110-α wild-type or the activating mutations E545K and H1047R was assayed by WST-1 after 72 h of NVP-BEZ235 and trastuzumab treatment at increasing concentrations. Oncogenic mutations conferred resistance to trastuzumab but were equally sensitive to NVP-BEZ235 compared with p110-α overexpressing or control cells. *, $P < 0.05$, compared with empty vector control. *C,* the growth of BT474 cells overexpressing either wild-type p110-α or hotspot mutations was assessed by crystal violet after 8 days of treatment. Mutated cells were less sensitive to trastuzumab (*T,* 15 nmol/L) compared with p110-α–overexpressing cells or mock control, whereas they were inhibited by NVP-BEZ235 (*B,* 10 nmol/L). **, $P < 0.01$ ***, $P < 0.001$, compared with mock control.

P-Akt was reduced at 1 hour post-dosing, but recovered to baseline 24 hours after drug administration (Figs. 5*B* and 6). P-S6 was also reduced at 1 hour post-dosing, but after 24 hours of treatment, P-S6 levels remained lower in H1047R tumors. The percentage of Ki67-positive cells decreased in NVP-BEZ235–treated animals at 1 hour after last drug administration, an effect that persisted 24 hours after the last dosage only in H1047R tumors (Fig. 5*C*). P-4EBP1 was not significantly changed by immunohistochemistry (data not shown).

In the same mice, we performed immunohistochemistry for levels of P-Akt, P-S6, and P-4EBP1 in normal skin at 1 hour after last drug administration. In the basal layer of skin, P-Akt, P-S6, and P-4EBP1 were significantly reduced upon NVP-BEZ235 treatment, 1 hour after last drug administration (Fig. 6*A* and *B*). These findings are similar to those observed in the tumors and suggest that skin may be a good surrogate tissue to study PI3K and mTOR inhibition.

Discussion

NVP-BEZ235 is an ATP competitor that potently and reversibly reduces the kinase activity of both p110 and mTOR. Consequently, it inhibits several PI3K pathway effectors, among them the serine/threonine-specific protein kinase Akt, the ribosomal protein S6, and the eukaryotic translation initiation factor 4E binding protein 1 (4EBP1) and induces nuclear translocation of forkhead transcription factor FKHRL1 (FOXO3a). The reported IC_{50}s for Thr308-P-Akt and Ser473-P-Akt are 29 and 8 nmol/L, respectively, and 6.5 nmol/L for mTOR (26). In our hands, the cellular IC_{50} for Akt phosphorylation measured by Western blot was significantly higher than that previously reported in the literature. This may be explained by differences in the assays employed, the cell lines tested and the durations of treatment. Also, the fact that p70 S6K, the upstream kinase of S6 ribosomal protein, is sequentially activated by both mTORC1 and PDK1 may explain why S6 phosphorylation is more sensitive to NVP-BEZ235 than Ser473-P-Akt (activated only by mTORC2). Thus, the inactivation of p70S6K may be an additive effect because its two major activator kinases are blocked by NVP-BEZ235. Furthermore, the disruption of the p70 S6K–IRS-1 feedback could explain, at least in part, an overall increase in Akt phosphorylation at times/concentrations when p70 S6K is inhibited. This effect varies between cell lines and over time. In DU145 prostate cancer cells, the IGF-IR tyrosine kinase inhibitor NVP-AEW541 was effective in preventing the Akt phosphorylation caused by both NVP-BEZ235 and everolimus, indicating that blocking upstream signaling may prevent the effects of negative

feedback loop disruption in these cells. Higher doses of NVP-BEZ235 (500 nmol/L) are also sufficient to fully prevent this increased upstream signaling. On the contrary, in BT474 and MDA-468 cells, IGF-IR inhibition did not revert the P-Akt induction seen at low doses of the dual inhibitor, leading us to postulate that alternative mechanisms could also account for the increased P-Akt (Supplementary Fig. S2). This observation has clinical implications because some patients treated with rapamycin analogues showed an increase in P-Akt in tumors and thus this effect has been postulated to be one of the reasons for their lack of clinical activity (32, 34). Therefore, it may be desirable to achieve dual inhibition of both mTOR and p110 in order to prevent this increase in P-Akt, which is reached by NVP-BEZ235 in the tested cells at doses >500 nmol/L.

In our studies, we found a lack of correlation between basal activity of the PI3K/Akt pathway and biochemical activity of NVP-BEZ235. It could be an indication that this agent blocks Akt in full regardless of its level of activation, in a similar fashion as it occurs with other kinase inhibitors such as lapatinib in erbB2-positive tumors. It is already known that in breast cancer, the activity of the PI3K/mTOR axis is often regulated by other signaling elements, such as HER2 overexpression or PTEN loss of function, which generally results in high levels of P-Akt. In agreement with this, we found that MDA-468 (PTEN−), BT474, and SkBr3 (both HER2+) have high levels of P-Akt. Because PI3K behaves as a "bottleneck" in which these and other pathways converge, a plausible explanation is that inhibiting PI3K with NVP-BEZ235 prevents Akt activation independently of the upstream pathways involved. This would support the lack of correlation between the compound's biochemical activity and basal levels of P-Akt. Regardless of the cause, this is an important observation because this data suggests that in patients, therapy with NVP-BEZ235 should not be selected based on the basal levels of P-Akt in the tumors.

NVP-BEZ235 blocked proliferation in all of the cancer cell lines tested (n = 21), independently of their PI3K pathway mutation status. In addition, NVP-BEZ235 was superior to everolimus in all tested cell lines. The differential sensitivity to the dual pan-PI3K/mTOR inhibitor (NVP-BEZ235) versus the allosteric mTORC1 inhibitor (everolimus) is likely to be due to the different mechanisms of action of these two agents. We believe that the higher activity of NVP-BEZ235 is due to inhibition of p110. At low doses, both compounds inhibit mTOR signaling and mTOR-dependent proliferation. At higher doses, everolimus' antiproliferative effects reach a plateau whereas the dual inhibitor continues to increase its antiproliferative effects that are maximal at higher concentrations (≥100 nmol/L). Importantly, inhibition of P-Thr308-Akt by NVP-BEZ235 also occurs at concentrations ≥100 nmol/L, suggesting that the increased antiproliferative activity of NVP-BEZ235 is due to PI3K inhibition (Supplementary Fig. S1).

In terms of any relationship between K-Ras mutations and sensitivity to NVP-BEZ235, we observed that MDA-231 cells, harboring a K-Ras mutation, responded poorly to NVP-BEZ235, suggesting that K-Ras mutation could signal for resistance to the dual inhibitor. Consequently, we studied a possible correlation between sensitivity to NVP-BEZ235 and mutation status in a panel of 27 cancer cell lines. We found that cell lines harboring either

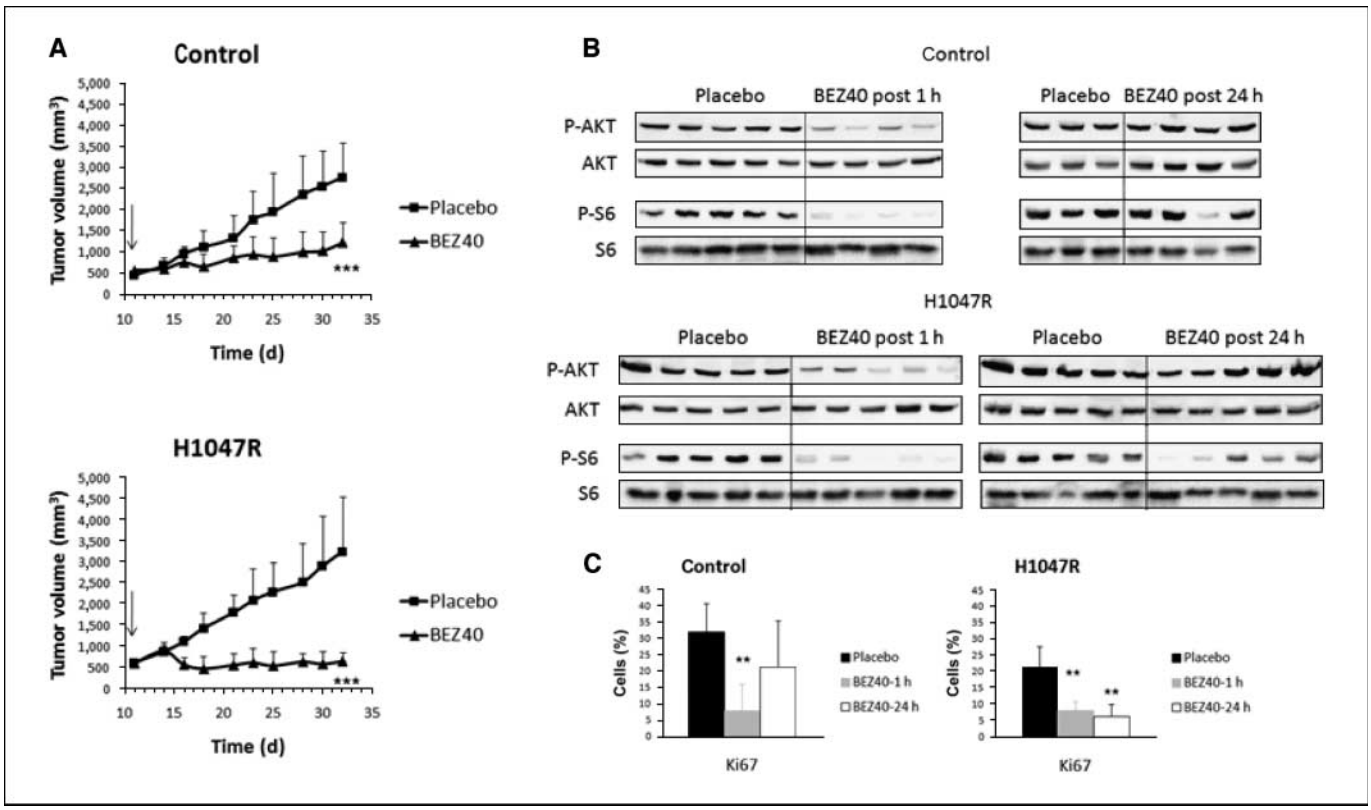

Figure 5. NVP-BEZ235 inhibits tumor growth of HER2+ BT474 xenografts overexpressing the H1047R mutation. *A,* mice were treated with a daily dose of NVP-BEZ235 of 40 mg/kg (*BEZ40*) or with vehicle alone (*Placebo*) for 21 d and tumors measured every 3 d. Groups were compared at the end of treatment (day 32). *Points,* mean; *bars,* SD. ***, $P < 0.001$. *Arrows,* start of treatment. *B,* Western blot of the BT474 xenografts from *A*. P-Akt and P-S6 levels were assessed 1 and 24 h after the last drug administration. Total Akt and S6, loading controls. *C,* quantification of Ki67 immunostaining of the same tumors.

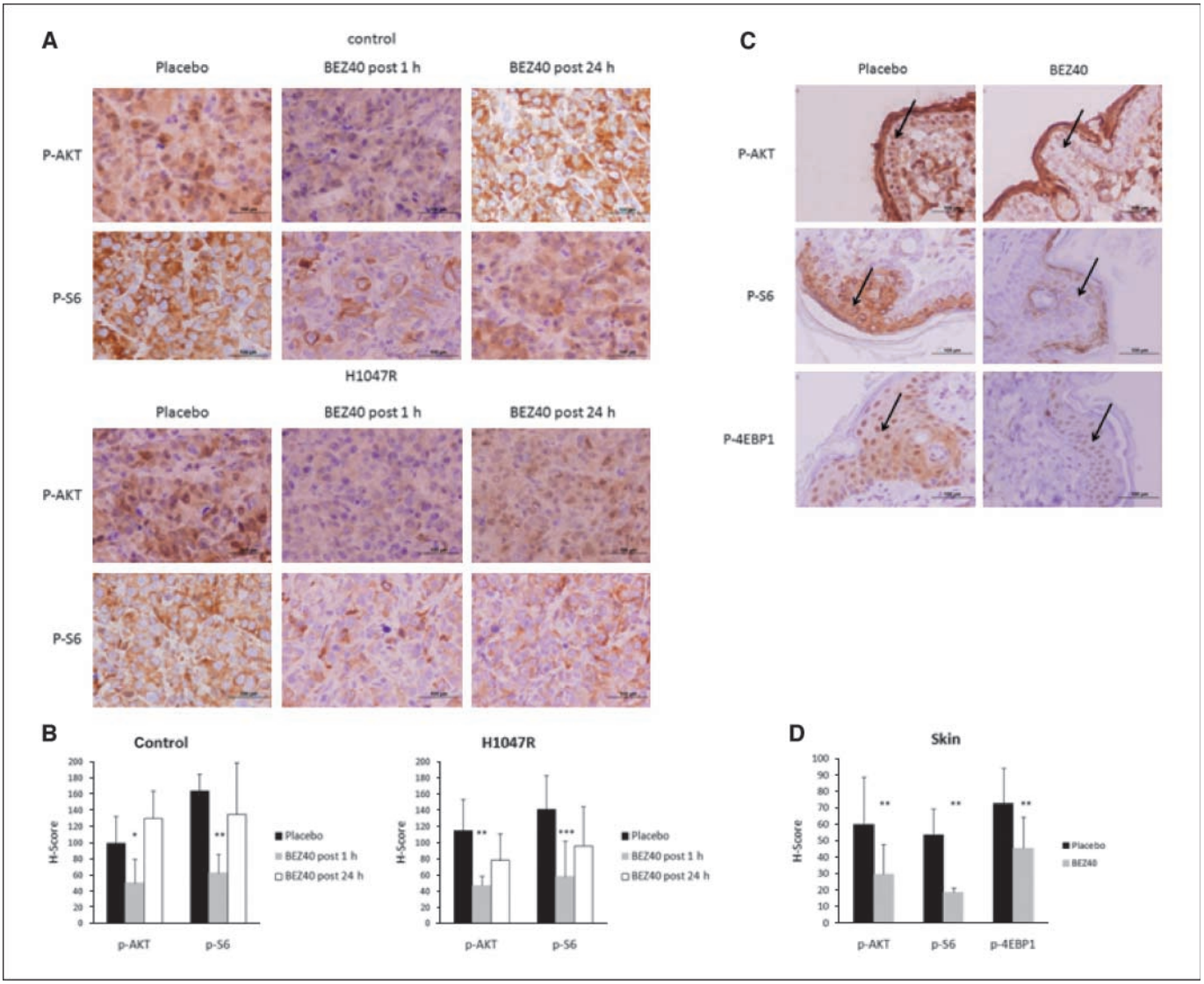

Figure 6. NVP-BEZ235 decreases P-Akt and P-S6 in tumor xenografts and mouse skin. *A,* representative examples of immunohistochemistry staining for P-Akt and P-S6 in tumor xenografts from Fig. 5, showing a decrease of the phosphorylation 1 h after last drug administration and their recovery 24 h thereafter. *B,* H-score quantification of *A*. *Columns,* mean; *bars,* SD. *C,* representative examples of immunohistochemistry staining for P-Akt, P-S6, and P-4EBP1 in skin of animals used in Fig. 5, 1 h after last drug administration. *Arrows,* basal layer of skin. *D,* H-score quantification of the same markers. *Columns,* mean; *bars,* SD; *, $P < 0.05$, **, $P < 0.01$, ***, $P < 0.001$.

K-Ras or B-Raf mutations, or EGFR amplification were slightly less sensitive to NVP-BEZ235 than the rest of the tested cells. Nevertheless, the GI_{50}s were relatively low (between 5 and 30 nmol/L) for all the tested cell lines. This may be explained by the predominant mTOR-inhibitory activity of NVP-BEZ235 we have observed in this concentration range (Fig. 1*A*).

NVP-BEZ235 equally targets wild-type and mutated p110-α. Maira and colleagues reported similar IC_{50}s for wild-type 110-α and the oncogenic mutations E545K and H1047R in enzyme assays, likely due to the fact that these mutations do not interfere with the ATP-binding pocket, where the drug reversibly binds.[5] Here, we have shown that NVP-BEZ235 reduced PI3K pathway activity in either p110-α wild-type or endogenously mutated cells. Moreover, NVP-BEZ235 targets the E545K and H1047R hotspot mutations when overexpressed in a cell line with low P-Akt levels (MDA-231), indicating that the use of this drug is appropriate for tumors harboring p110-α mutations. The observed inhibition of the PI3K pathway occurred in parallel to reduced cellular proliferation, potent G_1 arrest and increased expression of apoptotic markers such as cleaved caspase 3 and cleaved PARP.

The fact that NVP-BEZ235 targets both wild-type and mutated p110-α has important implications. Increased signaling of PI3K may occur via upstream or lateral activation (such as via receptor signaling or PTEN loss of function) or by the presence of activating mutations in PI3K itself. It is likely that inhibition of this pathway in any of these circumstances results in similar antiproliferative effects. Thus, an agent such as NVP-BEZ235 that can effectively target both wild-type and mutated p110-α has the potential for wider applicability in the clinic.

As an example, it has been shown that some HER2-positive patients are refractory to the anti-HER2 monoclonal antibody

[5] C. Garcia-Echeverria, personal communication.

trastuzumab due to the presence of oncogenic mutations in p110-α or PTEN loss (19). We have observed trastuzumab resistance by overexpressing the E545K and H1047R hotspot mutations in two HER2-amplified cell lines (BT474 and SkBr3 cells). This intrinsic resistance to trastuzumab was overcome by NVP-BEZ235, which showed similar activity in cells bearing either wild-type or mutated p110-α and was able to inhibit the phosphorylation of Akt in all cells.

The antitumor activity of NVP-BEZ235 was also evaluated *in vivo* using a xenograft model of BT474-derived cells overexpressing either the p110-α H1047R oncogenic mutation or an empty vector (mock control). NVP-BEZ235 significantly reduced tumor growth of both H1047R and empty vector control xenografts. Interestingly, in our hands, the H1047R-overexpressing tumors responded better to the treatment. We could speculate that this increased response was due to a sustained P-S6 suppression and reduced proliferation (Ki67 low) throughout the whole treatment period.

Nowadays, the identification of potential biomarkers is of tremendous importance as targeted therapeutics evolve. These biomarkers aim to serve as surrogates that can correlate drug activity and target down-regulation. For this reason, we have quantified P-Akt, P-S6, P-4EBP1 and the percentage of Ki67 positive cells, in tumor xenografts and mouse skin, as end points to assess *in vivo* NVP-BEZ235 activity. The levels of P-Akt and P-S6RP were significantly reduced 1 hour after NVP-BEZ235 dosage both in tumor xenografts and skin, suggesting that the latter could be used as a surrogate marker of target down-regulation in patients treated with NVP-BEZ235.

The present work shows that NVP-BEZ235 specifically inhibits activated signaling in both wild-type and mutated p110-α, both in cellular models and in xenografts. Importantly, inhibition of p110 and mTOR signaling consistently offers an antiproliferative advantage than inhibiting mTOR alone. Taken together with the work by Maira and colleagues, in which NVP-BEZ235 showed activity in cells with PTEN loss, our observations offer a valid therapeutic alternative for the treatment of solid tumors with mutated PI3K.

Disclosure of Potential Conflicts of Interest

M. Maira: shareholder, Novartis Pharma, AG. J. Baselga: Speaker's Bureau/honoraria, Novartis Pharma, AG. The other authors disclosed no potential conflicts of interest.

Acknowledgments

Received 4/14/2008; revised 6/21/2008; accepted 7/25/2008.

Grant support: Breast Cancer Research Foundation.

The costs of publication of this article were defrayed in part by the payment of page charges. This article must therefore be hereby marked *advertisement* in accordance with 18 U.S.C. Section 1734 solely to indicate this fact.

We thank Dr. Joan Seoane for helpful discussion and revision of the manuscript and Dr. Julià Blanco (Hospital Universitari Germans Trias i Pujol) for granting us access to an S2 facility.

References

1. Samuels Y, Wang Z, Bardelli A, et al. High frequency of mutations of the PIK3CA gene in human cancers. Science 2004;304:554.
2. Bachman KE, Argani P, Samuels Y, et al. The PIK3CA gene is mutated with high frequency in human breast cancers. Cancer Biol Ther 2004;3:772–5.
3. Lee JW, Soung YH, Kim SY, et al. PIK3CA gene is frequently mutated in breast carcinomas and hepatocellular carcinomas. Oncogene 2005;24:1477–80.
4. Campbell IG, Russell SE, Choong DY, et al. Mutation of the PIK3CA gene in ovarian and breast cancer. Cancer Res 2004;64:7678–81.
5. Levine DA, Bogomolniy F, Yee CJ, et al. Frequent mutation of the PIK3CA gene in ovarian and breast cancers. Clin Cancer Res 2005;11:2875–8.
6. Philp AJ, Campbell IG, Leet C, et al. The phosphatidylinositol 3′-kinase p85α gene is an oncogene in human ovarian and colon tumors. Cancer Res 2001;61:7426–9.
7. Vanhaesebroeck B, Waterfield MD. Signaling by distinct classes of phosphoinositide 3-kinases. Exp Cell Res 1999;253:239–54.
8. Cantley LC. The phosphoinositide 3-kinase pathway. Science 2002;296:1655–7.
9. Yu J, Zhang Y, McIlroy J, Rordorf-Nikolic T, Orr GA, Backer JM. Regulation of the p85/p110 phosphatidylinositol 3′-kinase: stabilization and inhibition of the p110α catalytic subunit by the p85 regulatory subunit. Mol Cell Biol 1998;18:1379–87.
10. Rodriguez-Viciana P, Sabatier C, McCormick F. Signaling specificity by Ras family GTPases is determined by the full spectrum of effectors they regulate. Mol Cell Biol 2004;24:4943–54.
11. Alessi DR, James SR, Downes CP, et al. Characterization of a 3-phosphoinositide-dependent protein kinase which phosphorylates and activates protein kinase Bα. Curr Biol 1997;7:261–9.
12. Sarbassov DD, Guertin DA, Ali SM, Sabatini DM. Phosphorylation and regulation of Akt/PKB by the rictor-mTOR complex. Science 2005;307:1098–101.
13. Engelman JA, Luo J, Cantley LC. The evolution of phosphatidylinositol 3-kinases as regulators of growth and metabolism. Nat Rev Genet 2006;7:606–19.
14. Inoki K, Li Y, Zhu T, Wu J, Guan KL. TSC2 is phosphorylated and inhibited by Akt and suppresses mTOR signalling. Nat Cell Biol 2002;4:648–57.
15. Liaw D, Marsh DJ, Li J, et al. Germline mutations of the PTEN gene in Cowden disease, an inherited breast and thyroid cancer syndrome. Nat Genet 1997;16:64–7.
16. Vogt PK, Kang S, Elsliger MA, Gymnopoulos M. Cancer-specific mutations in phosphatidylinositol 3-kinase. Trends Biochem Sci 2007;32:342–9.
17. Samuels Y, Diaz LA, Jr., Schmidt-Kittler O, et al. Mutant PIK3CA promotes cell growth and invasion of human cancer cells. Cancer Cell 2005;7:561–73.
18. Bader AG, Kang S, Vogt PK. Cancer-specific mutations in PIK3CA are oncogenic *in vivo*. Proc Natl Acad Sci U S A 2006;103:1475–9.
19. Berns K, Horlings HM, Hennessy BT, et al. A functional genetic approach identifies the PI3K pathway as a major determinant of trastuzumab resistance in breast cancer. Cancer Cell 2007;12:395–402.
20. Chakravarti A, Zhai G, Suzuki Y, et al. The prognostic significance of phosphatidylinositol 3-kinase pathway activation in human gliomas. J Clin Oncol 2004;22:1926–33.
21. Clark AS, West K, Streicher S, Dennis PA. Constitutive and inducible Akt activity promotes resistance to chemotherapy, trastuzumab, or tamoxifen in breast cancer cells. Mol Cancer Ther 2002;1:707–17.
22. Hu L, Hofmann J, Lu Y, Mills GB, Jaffe RB. Inhibition of phosphatidylinositol 3′-kinase increases efficacy of paclitaxel in *in vitro* and *in vivo* ovarian cancer models. Cancer Res 2002;62:1087–92.
23. Brognard J, Clark AS, Ni Y, Dennis PA. Akt/protein kinase B is constitutively active in non-small cell lung cancer cells and promotes cellular survival and resistance to chemotherapy and radiation. Cancer Res 2001;61:3986–97.
24. Nagata Y, Lan KH, Zhou X, et al. PTEN activation contributes to tumor inhibition by trastuzumab, and loss of PTEN predicts trastuzumab resistance in patients. Cancer Cell 2004;6:117–27.
25. Marone R, Cmiljanovic V, Giese B, Wymann MP. Targeting phosphoinositide 3-kinase: moving towards therapy. Biochim Biophys Acta 2008;1784:159–85.
26. Maira S-M SF, Brueggen J, et al. Identification and characterization of NVP-BEZ235, a new orally available dual PI3K/mTor inhibitor with potent *in vivo* antitumor activity. Mol Cancer Ther. In press 2008.
27. Baselga J, Norton L, Albanell J, Kim YM, Mendelsohn J. Recombinant humanized anti-HER2 antibody (Herceptin) enhances the antitumor activity of paclitaxel and doxorubicin against HER2/neu overexpressing human breast cancer xenografts. Cancer Res 1998;58:2825–31.
28. Guertin DA, Stevens DM, Thoreen CC, et al. Ablation in mice of the mTORC components raptor, rictor, or mLST8 reveals that mTORC2 is required for signaling to Akt-FOXO and PKCα, but not S6K1. Dev Cell 2006;11:859–71.
29. Stolovich M, Tang H, Hornstein E, et al. Transduction of growth or mitogenic signals into translational activation of TOP mRNAs is fully reliant on the phosphatidylinositol 3-kinase-mediated pathway but requires neither S6K1 nor rpS6 phosphorylation. Mol Cell Biol 2002;22:8101–13.
30. Neshat MS, Mellinghoff IK, Tran C, et al. Enhanced sensitivity of PTEN-deficient tumors to inhibition of FRAP/mTOR. Proc Natl Acad Sci U S A 2001;98:10314–9.
31. Harrington LS, Findlay GM, Gray A, et al. The TSC1-2 tumor suppressor controls insulin-PI3K signaling via regulation of IRS proteins. J Cell Biol 2004;166:213–23.
32. O'Reilly KE, Rojo F, She QB, et al. mTOR inhibition induces upstream receptor tyrosine kinase signaling and activates Akt. Cancer Res 2006;66:1500–8.
33. Sarbassov DD, Ali SM, Sengupta S, et al. Prolonged rapamycin treatment inhibits mTORC2 assembly and Akt/PKB. Mol Cell 2006;22:159–68.
34. Tabernero J, Rojo F, Calvo E, et al. Dose- and schedule-dependent inhibition of the mammalian target of rapamycin pathway with everolimus: a phase I tumor pharmacodynamic study in patients with advanced solid tumors. J Clin Oncol 2008;26:1603–10.

NVP-BEZ235, a Dual PI3K/mTOR Inhibitor, Prevents PI3K Signaling and Inhibits the Growth of Cancer Cells with Activating PI3K Mutations

Violeta Serra, Ben Markman, Maurizio Scaltriti, et al.

Cancer Res 2008;68:8022-8030.